Chiral symmetry breaking in a semilocalized magnetic field

Gaoqing Cao

School of Physics and Astronomy, Sun Yat-Sen University, Guangzhou 510275, China
and Department of Physics and Center for Particle Physics and Field Theory,
Fudan University, Shanghai 200433, China

(Received 8 January 2018; published 19 March 2018)

In this work, we explore the pattern of chiral symmetry breaking and restoration in a solvable magnetic field configuration within the Nambu–Jona-Lasinio model. The special semilocalized static magnetic field can roughly mimic the realistic situation in peripheral heavy ion collisions; thus, the study is important for the dynamical evolution of quark matter. We find that the magnetic-field-dependent contribution from discrete spectra usually dominates over the contribution from continuum spectra and chiral symmetry breaking is locally catalyzed by both the magnitude and scale of the magnetic field. The study is finally extended to the case with finite temperature or chemical potential.

DOI: 10.1103/PhysRevD.97.054021

I. INTRODUCTION

Recently, it was found that an extremely strong electromagnetic (EM) field can be generated in peripheral relativistic heavy-ion collisions (HICs), such as those at the Relativistic Heavy Ion Collider (RHIC) at BNL and the Large Hadron Collider (LHC) at CERN [1–4]. Relevantly, an unexpected inverse magnetic catalysis effect (IMCE) was discovered at finite temperature from lattice quantum chromodynamics (LQCD) simulations [5–8]. In this context, much effort was devoted to explaining or exploring the thermodynamic properties of strong coupling systems in the presence of a constant magnetic field [9–17]; see review Ref. [18]. In addition, due to the successful realization of the chiral magnetic effect (CME) in the condensed matter system ZrTe5 [19], chiral anomaly phenomena [20,21] and the related phenomenology in hydrodynamics [22–24] become even hotter topics which further push the efforts to look for the CME signal in the QCD system, see reviews Refs. [25–28]. It is very interesting to note that the magnetic field usually brings us a lot of surprises due to the specific quantum effects.

One thing should be kept in mind about the HICs is that the magnetic field produced is actually inhomogeneous in the fireball. Thus, it is very important to explore how the free energy and chiral symmetry will be affected by such a magnetic field, and that exploration is the main goal of this work. A sizable electric field can also be generated in HICs on an event-by-event basis, due to the proton fluctuation in the colliding ions. However, the average is small over many events for the same ion collisional systems, and the magnetic field perpendicular to the reaction plane dominates for a larger impact parameter [4]. Thus, we just focus on the effect of the magnetic field here. Surely, the configuration of the magnetic field is quite complicated in the fireball because of the initial charge fluctuation and later expansion of the fireball, but the main feature can be captured by the configuration between the two long straight electric currents with opposite directions [4]. In order to derive an exact fermion propagator for later use, we choose an ideal semilocalized configuration, that is $\vec{B}(x) = B\mathrm{sech}^2(x/\lambda)\hat{z}$ [29,30], which is illuminated in Fig. 1. As we can see, the corresponding electric current configuration is mainly composed of two peaks along opposite directions which is just like the case in peripheral heavy ion collisions. The contribution of fermions to the free energy in such a magnetic field was studied in detail in both $2+1$ [29] and

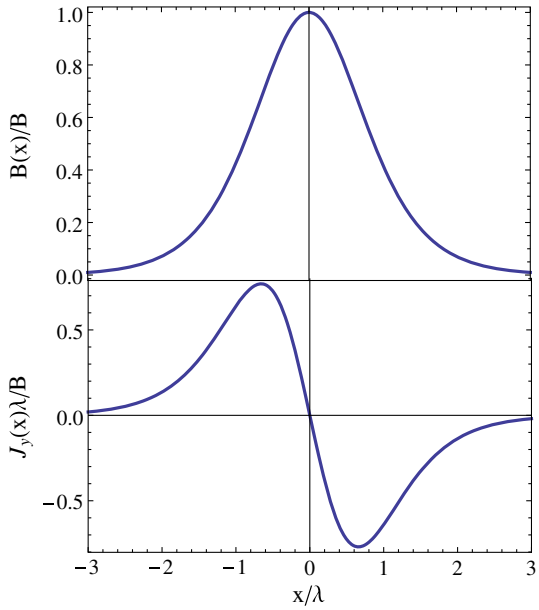

FIG. 1. The configurations of the semilocalized magnetic field $B(x) = B\mathrm{sech}^2(x/\lambda)$ along z direction and the corresponding current $J_y = B'(x)$ along y direction in the region $(-3\lambda, 3\lambda)$.

$3+1$ dimensions [30], but the simple results [see Eqs. (13) and (14)] should be treated cautiously since the quadratic terms of B were not dropped completely. Quite recently, the Schwinger mechanism was checked, and pair production was found to be enhanced in such a magnetic field together with the presence of a parallel electric field [31].

In this work, we only focus on the pure magnetic field case for simplicity, and the paper is arranged as follows: In Sec. II, we develop the main formalism for a semilocalized magnetic field within the Nambu–Jona-Lasinio (NJL) model, where Sec. II A is devoted to a preliminary calculation of the thermodynamic potential of fermion systems, with the assumption of a constant mass gap, and Sec. II B is devoted to exploring the pattern of chiral symmetry breaking in the weak magnetic field approximation. The main numerical results for both the constant and semilocalized mass gap *Ansätze* are given in Sec. III. Finally, we briefly summarize in Sec. IV.

II. NAMBU–JONA-LASINIO MODEL WITH A SEMILOCALIZED MAGNETIC FIELD

In order to study the effect of a semilocalized magnetic field to the chiral symmetry breaking and restoration in QCD systems, we adopt the effective Nambu–Jona-Lasinio model [32–34] which has an approximate chiral symmetry as the basic QCD theory. Taking into account the magnetic field $B(x)$ and baryon chemical potential μ, the Lagrangian is given by

$$\mathcal{L}=\bar{\psi}(i\not{D}-m_0+\mu\gamma^0)\psi+G[(\bar{\psi}\psi)^2+(\bar{\psi}i\gamma^5\boldsymbol{\tau}\psi)^2], \quad (1)$$

where $\psi=(u,d)^T$ is the two-flavor quark field, $\boldsymbol{\tau}$ are Pauli matrices in flavor space, m_0 is the current quark mass, and G is the coupling constant with a dimension $[\mathrm{GeV}^{-2}]$. Here, $D_\mu=\partial_\mu+iqA_\mu$ is the covariant derivative in flavor space with electric charges $q_u=2e/3$ and $q_d=-e/3$ for the u and d quarks, and the static magnetic field is chosen to be along the z direction but varying along the x direction with the corresponding vector potential given by $A_\mu=(0,0,-B\lambda\tanh(x/\lambda),0)$ [29].

In order to explore the ground state of the system, we introduce four auxiliary fields $\sigma=-2G\bar{\psi}\psi$ and $\boldsymbol{\pi}=-2G\bar{\psi}i\gamma^5\boldsymbol{\tau}\psi$, then the Lagrangian density becomes

$$\mathcal{L}=\bar{\psi}[i\not{D}-m_0-\sigma-i\gamma^5(\tau_3\pi_0+\tau_\pm\pi_\pm)+\mu\gamma^0]\psi-\frac{\sigma^2+\pi_0^2+\pi_\mp\pi_\pm}{4G}, \quad (2)$$

where $\pi_\pm$ are the physical fields which are related to the auxiliary fields as $\pi_\pm=(\pi_1\mp i\pi_2)/\sqrt{2}$, and $\tau_\pm=(\tau_1\pm i\tau_2)/\sqrt{2}$ are the raising and lowering operators in flavor space, respectively. The order parameters for the spontaneous breaking of $SU_L(3)\times SU_R(3)$ chiral symmetry are the expectation values of the collective fields $\langle\sigma\rangle$, $\langle\pi_0\rangle$, and $\langle\pi_\pm\rangle$. There should be no pion superfluid for vanishing isospin chemical potential, that is, $\langle\pi_\pm\rangle=0$, in the recent case. But there might exist a stable π^0 domain wall due to the coupling term $\mu\mathbf{B}\cdot\boldsymbol{\nabla}\boldsymbol{\pi}^{\mathbf{0}}(\mathbf{x})$ when B exceeds the critical value $(0.255\ \mathrm{GeV})^2$ in nuclear matter [35]. Although we can show the possibility of the π^0 domain wall in the NJL model by expanding over small $\pi^0(x)$, the calculation is so involved that we just neglect it in this work. It is more reasonable to assume a spatial varying chiral condensate for an inhomogeneous magnetic field, so we just set $\langle\sigma\rangle=m+m(x)-m_0$. Then by integrating out the fermion degrees of freedom, the partition function can be expressed as a bosonic version:

$$\begin{aligned}\mathcal{Z}=&\int[D\hat{\sigma}][D\hat{\pi}_0][D\hat{\pi}_\pm]\\&\times\exp\Bigg\{-\int d^4X\left[\frac{(m+m(x)-m_0+\hat{\sigma})^2+\hat{\pi}_0^2+\hat{\pi}_\pm^2}{4G}\right]\\&+\mathrm{Tr}\ln[i\not{D}-m-m(x)-\hat{\sigma}-i\gamma^5(\tau_3\hat{\pi}_0+\tau_\pm\hat{\pi}_\pm)\\&+\mu\gamma^0]\Bigg\}, \end{aligned}\quad (3)$$

where the fields with a hat denote the bosonic fluctuation modes, and the trace is taken over the quark spin, flavor, color, and the spacetime coordinate spaces. In the mean-field approximation, the thermodynamic potential can be expressed as

$$\Omega=\frac{1}{V_4}\left\{\int d^4X\frac{(m+m(x)-m_0)^2}{4G}-\mathrm{Tr}\ln[i\not{D}-m-m(x)+\mu\gamma^0]\right\}, \quad (4)$$

where the four-dimensional volume is $V_4=\beta V$, with $\beta=1/T$ the inverse temperature, and V as the spatial volume of the system. In principle, the gap equation can be obtained by the extremal condition $\delta\Omega/\delta m(x)=0$ as

$$\int d^3X\frac{m+m(x)-m_0}{2G}-\mathrm{Tr}_3\mathcal{S}_A(x)=0, \quad (5)$$

where the fermion propagator in the semilocalized magnetic field is given by $\mathcal{S}_A(x)=-[i\not{D}-m-m(x)+\mu\gamma^0]^{-1}$, and the coordinate integrals take over all directions but x. The gap equation can be separated into two parts: the x-independent part which gives the expectation value of m and the x-dependent part which gives the expectation value of $m(x)$. It is not easy to solve the gap equation for spatially varying $m(x)$ such as the inhomogeneous FFLO phases [36–40], let alone that the explicit form of $m(x)$ is unknown. For this reason, we first develop a formalism with only constant m (that is $m(x)=0$) to evaluate the thermodynamic potential in the semilocalized magnetic field and then explore small $m(x)$ by adopting the Taylor expansion in the weak magnetic field limit.

A. Thermodynamic potential with constant m

It is usually not easy to solve the Dirac equation exactly in the presence of an inhomogeneous magnetic field. But for the chosen semilocalized magnetic field $B(x) = B\mathrm{sech}^2(x/\lambda)$ with B the magnitude and λ the scale, we are able to derive an exact solution [29,30]. Because the magnetic field is well confined in the region $(-3\lambda, 3\lambda)$ as shown in Fig. 1, we will first choose $L = 6\lambda$ as the system size to study the change of the thermodynamic potential due to the presence of the inhomogeneous magnetic field. One can also understand it in another way; that is, the magnetic field spreads all over the space with the centers at $x_0 = 6n\lambda$, $(n \in \mathbb{Z})$, then the situation is just equal to the case with a system size $L = 6\lambda$ due to the periodicity of the configuration. After developing the whole formalism, we simply extend the formula to the system with a fixed size.

For brevity, we will proceed with one color and one flavor first. By following the discussions in Ref. [29,30], the discrete eigenenergy for a given charge q_f in the orthogonal dimensions can be presented as

$$\epsilon_{ns}(p_2) = \left[p_2^2 + (q_\mathrm{f}B\lambda)^2 - \lambda^{-2}\left(n + \frac{1}{2} - c_s\right)^2 - (p_2 q_\mathrm{f} B\lambda^2)^2\left(n + \frac{1}{2} - c_s\right)^{-2}\right]^{1/2}, \tag{6}$$

where $c_s = |\frac{1}{2} + sq_\mathrm{f}B\lambda^2|$ with $s = \pm$ denoting the fermion spin along the z direction and n constrained to $0 \le n \le N_s$ with $N_s = \mathrm{ceiling}(c_s - \frac{3}{2} - \sqrt{|p_2 q_\mathrm{f} B\lambda^3|})$. One should notice that in the constant magnetic field limit $\lambda \to \infty$, $\epsilon_{ns}(p_2) = [(2n + 1 - s\mathrm{sgn}(q_\mathrm{f}B))|q_\mathrm{f}B|]^{1/2}$ and $N_s \to \infty$ for a fixed p_2. Besides, there are also contributions from the continuum spectra as we will illuminate soon.

In the case with finite temperature and density, the contribution of the fermion loop to the thermodynamic potential can be given as

$$\begin{aligned}\Omega(m^2, q_\mathrm{f}, B, \lambda) &= -\frac{1}{2L}\int\frac{d^3p}{(2\pi)^2}\mathrm{Tr}\ln[-\partial_x^2 + V_{p_2}(x) + m^2 + p_3^2 + (\omega_l + i\mu)^2] \\ &= -\frac{1}{2L}\int\frac{d^3p}{(2\pi)^2}\int dm^2\mathrm{Tr}[-\partial_x^2 + V_{p_2}(x) + m^2 + p_3^2 + (\omega_l + i\mu)^2]^{-1} \\ V_{p_2}(x) &= -\lambda^{-2}\left[\left(\frac{1}{2} + q_\mathrm{f}B\lambda^2\sigma_3\right)^2 - \frac{1}{4}\right]\times\left[1 - \tanh^2\left(\frac{x}{\lambda}\right)\right] + \sum_{t=\pm}\frac{1}{2}(p_2 - tq_\mathrm{f}B\lambda)^2\left[1 + t\tanh\left(\frac{x}{\lambda}\right)\right],\end{aligned} \tag{7}$$

where the fermion Matsubara frequency $\omega_l = (2l + 1)\pi T(l \in \mathbb{Z})$, and we denote $\int d^3p = \int dp_2 dp_3 T\sum_{l=-\infty}^{\infty}$ for convenience. Then, the trace of the Green's function can be completed with the help of hypergeometric functions to give

$$\begin{aligned}&\Omega(m^2, q_\mathrm{f}, B, \lambda) \\ &= \frac{\lambda^2}{4L}\int\frac{d^3p}{(2\pi)^2}\int dm^2\sum_{s,t=\pm}\left(\frac{1}{\alpha_+} + \frac{1}{\alpha_-}\right)\times\psi\left(\frac{1}{2}(\alpha_+ + \alpha_- + 1) - tc_s\right) \\ &= \frac{1}{L}\int\frac{d^3p}{(2\pi)^2} \\ &\quad\times\int dm^2\sum_{s,t=\pm}\frac{\partial_{(\omega_l + i\mu)^2}\Gamma(\frac{1}{2}(\alpha_+ + \alpha_- + 1) - tc_s)}{\Gamma(\frac{1}{2}(\alpha_+ + \alpha_- + 1) - tc_s)},\end{aligned} \tag{8}$$

where $\alpha_\pm = \lambda\sqrt{E_\pm^2(p_2, p_3, m) + (\omega_l + i\mu)^2}$ with the continuum spectrum $E_t(p_2, p_3, m) = \sqrt{(p_2 + tq_\mathrm{f}B\lambda)^2 + p_3^2 + m^2}$. Completing the summation over ω_l by deforming the integral contour and then the integral over m^2, we find the contribution from the bound states or discrete spectra is

$$\begin{aligned}&\Omega_b(m^2, q_\mathrm{f}, B, \lambda, T, \mu) \\ &= -\frac{1}{L}\int\frac{dp_2 dp_3}{(2\pi)^2}\int dm^2\sum_{s,t=\pm}\sum_{n=0}^{N_s}\frac{\tanh(\frac{E_{ns}(p_2, p_3, m) + t\mu}{2T})}{4E_{ns}(p_2, p_3, m)} \\ &= -\frac{1}{2L}\int\frac{dp_2 dp_3}{(2\pi)^2}\sum_{s,t=\pm}\sum_{n=0}^{N_s}[E_{ns} + 2T\ln(1 + e^{-(E_{ns} + t\mu)/T})],\end{aligned} \tag{9}$$

where the dispersion relation is $E_{ns}(p_2, p_3, m) = (\epsilon_{ns}^2(p_2) + p_3^2 + m^2)^{1/2}$. If the integral region of p_2 is fixed to $\pm q_\mathrm{f}BL/2$ with L the fixed system size, then in the constant magnetic field limit $\lambda \to \infty$, we can recover the unregularized form [15] of the thermodynamic potential from Eq. (9). The contribution from the cut branches $\pm E_t(p_2, p_3, m)$ can be evaluated with the help of the following integral transformation properties:

$$\begin{aligned}&\frac{1}{2\pi i}\int_{-\infty + i\eta}^{-a + i\eta} dx\frac{f(x^2)}{\sqrt{a^2 - x^2}}\tanh\left(\frac{x + \mu}{2T}\right) = \frac{1}{2\pi}\int_a^\infty dx\frac{f(x^2)}{\sqrt{x^2 - a^2}}\tanh\left(\frac{x - \mu}{2T}\right), \\ &\frac{1}{2\pi i}\int_{a + i\eta}^{\infty + i\eta} dx\frac{f(x^2)}{\sqrt{a^2 - x^2}}\tanh\left(\frac{x + \mu}{2T}\right) = \frac{1}{2\pi}\int_a^\infty dx\frac{f(x^2)}{\sqrt{x^2 - a^2}}\tanh\left(\frac{x + \mu}{2T}\right),\end{aligned} \tag{10}$$

with $a > 0$, $\eta \gtrless 0$. Then, the contribution from the continuum spectrum can be given as

$$\begin{aligned}\Omega_c(m^2,q_{\rm f},B,\lambda,T,\mu) &= \frac{\lambda}{16\pi L}\int\frac{dp_2dp_3}{(2\pi)^2}\int dm^2\sum_{s,t,u,v=\pm}\int_{E_t}^{\infty}d\omega\frac{1}{\sqrt{\omega^2-E_t^2}}\left[\tanh\left(\frac{\omega-\mu}{2T}\right)+\tanh\left(\frac{\omega+\mu}{2T}\right)\right]\\ &\times\psi\left(\frac{1}{2}(iv\lambda\sqrt{\omega^2-E_t^2}+\lambda\sqrt{|\omega^2-E_{-t}^2|}(iv\theta(\omega-E_{-t})+\theta(E_{-t}-\omega))+1)-u\left|\frac{1}{2}+sq_{\rm f}B\lambda^2\right|\right)\\ &= \frac{\lambda}{2\pi L}\int\frac{dp_2dp_3}{(2\pi)^2}\sum_{s,u,v=\pm}\int_0^{\infty}dy\left[\sqrt{y^2+E_\perp^2}+T\ln\left(1+e^{-(\sqrt{y^2+E_\perp^2}+\mu)/T}\right)+T\ln\left(1+e^{-(\sqrt{y^2+E_\perp^2}-\mu)/T}\right)\right]\\ &\times\psi\left(\frac{1}{2}(iv\lambda y+\lambda\sqrt{|h|}(iv\theta(h)+\theta(-h))+1)-u\left(\frac{1}{2}+sq_{\rm f}B\lambda^2\right)\right),\end{aligned}\tag{11}$$

where $h(y,p_2,q_{\rm f},B,\lambda)=y^2+4p_2q_{\rm f}B\lambda-4(q_{\rm f}B\lambda)^2$ and $E_\perp(p_2,p_3,m)=\sqrt{p_2^2+p_3^2+m^2}$. This actually cannot reduce to the well-known form in the vanishing magnetic field limit $B\to 0$ because some B-independent terms have been dropped in deriving Eq. (8) [29]. However, we can still recognize the main part of the thermodynamic potential with eigenenergy $E(p)=\sqrt{p^2+m^2}$ except for the multiplicative digamma function ψ.

For further convenience, we denote the vacuum and thermal parts of the thermodynamic potential $\Omega_{b/c}(m^2,q_{\rm f},B,\lambda,T,\mu)$ by $\Omega_{b/c}(m^2,q_{\rm f},B,\lambda)$ and $\Omega_{b/c}^t(m^2,q_{\rm f},B,\lambda,T,\mu)$, separately. The divergence comes solely from the vacuum part $\Omega_B=\Omega_b+\Omega_c$, and the B-dependent part was previously renormalized to a compact form by dropping some B-independent and B^2 terms [30]. Actually, for the study of chiral symmetry breaking and restoration, the B^2 terms can not be dropped at will because Ω_B will have a "wrong" sign compared to the case with constant magnetic field [15]:

$$\Omega_B=\frac{1}{8\pi^2}\int_0^{\infty}\frac{ds}{s^3}e^{-m^2s}\left(\frac{q_{\rm f}Bs}{\tanh(q_{\rm f}Bs)}-1\right).\tag{12}$$

Thus, from the $2+1$-dimensional result [29],

$$\begin{aligned}\Omega_B(m^2,q_{\rm f},B,\lambda) &= \frac{1}{2\pi\lambda^2L}\int_0^{\infty}\frac{dx}{e^{2\pi x}-1}\Re\left[(|q_{\rm f}B\lambda^2|-ix)g^{-1}(x)\right.\\ &\left.\times(\lambda^2m^2+g^2(x))\ln\frac{\lambda m-ig(x)}{\lambda m+ig(x)}\right],\end{aligned}\tag{13}$$

we should just keep the third momentum integral form for the $3+1$-dimensional case as [30]

$$\begin{aligned}\Omega_B(m^2,q_{\rm f},B,\lambda) &= \frac{1}{2\pi^2\lambda^2L}\int_0^{\infty}dp_3\int_0^{\infty}\frac{dx}{e^{2\pi x}-1}\Re\\ &\times\left[(|q_{\rm f}B\lambda^2|-ix)g^{-1}(x)(\lambda^2(m^2+p_3^2)\right.\\ &\left.+g^2(x))\ln\frac{\lambda\sqrt{m^2+p_3^2}-ig(x)}{\lambda\sqrt{m^2+p_3^2}+ig(x)}\right],\end{aligned}\tag{14}$$

where $g(x)=x^2+2ix|q_{\rm f}B\lambda^2|$. Then, $\Delta\Omega_B(m^2,q_{\rm f},B,\lambda)-\Delta\Omega_B(m_1^2,q_{\rm f},B,\lambda)$, where $\Delta\Omega$ denotes the difference between the finite magnetic field result and the one in the $B\to 0$ limit, can be shown to be convergent for $m_1\neq 0$ and negative divergent for $m_1=0$. Thus, $m\neq 0$ is always favored in the magnetic field.

Here, it is illuminative to present the thermodynamic potential for N species fermion systems in $2+1$ dimensions because it is renormalizable in the large-N expansion [41]. In the chiral limit, by following the renormalization scheme in Ref. [12], the thermodynamic potential can be presented as

$$\Omega/N=-\frac{m^2m_g}{2\pi}\mathrm{sgn}(g-g_c)+\frac{|m|^3}{3\pi}+\Delta\Omega_B,\tag{15}$$

where Ω_B is given by Eq. (13), m_g stands for the magnitude of the coupling g, and g_c is the critical coupling constant. One can easily check that $\Delta\Omega_B(m^2,q_{\rm f},B,\lambda)=0$ in the limit $\lambda\to 0$ as should be and the thermodynamic potential is reduced to

$$\begin{aligned}&\Omega(m^2,q_{\rm f},B,\lambda)/N\\ &= -\frac{m^2m_g}{2\pi}\mathrm{sgn}(g-g_c)+\frac{m^3}{3\pi}+\frac{\lambda}{2\pi L}\int_0^{\infty}\frac{dx}{x(e^{2\pi x}-1)}\Re\\ &\times\left[\sqrt{|q_{\rm f}B|x}\left((1+i)|q_{\rm f}B|x+\frac{1-i}{2}m^2\right)\right.\\ &\left.\times\ln\frac{m+(1-i)\sqrt{|q_{\rm f}B|x}}{m-(1-i)\sqrt{|q_{\rm f}B|x}}\right],\end{aligned}\tag{16}$$

in the limit $\lambda\to\infty$.

Turn back to the case with $3+1$ dimensions. For the thermal parts, it is clear that

$$\begin{aligned}&\lim_{B\to 0}\Omega_b^t(m^2,q_{\rm f},B,\lambda,T,\mu)=0,\\ &\lim_{B\to 0}\Omega_c^t(m^2,q_{\rm f},B,\lambda,T,\mu)\neq 0,\end{aligned}\tag{17}$$

so the pure B-dependent part can be given as

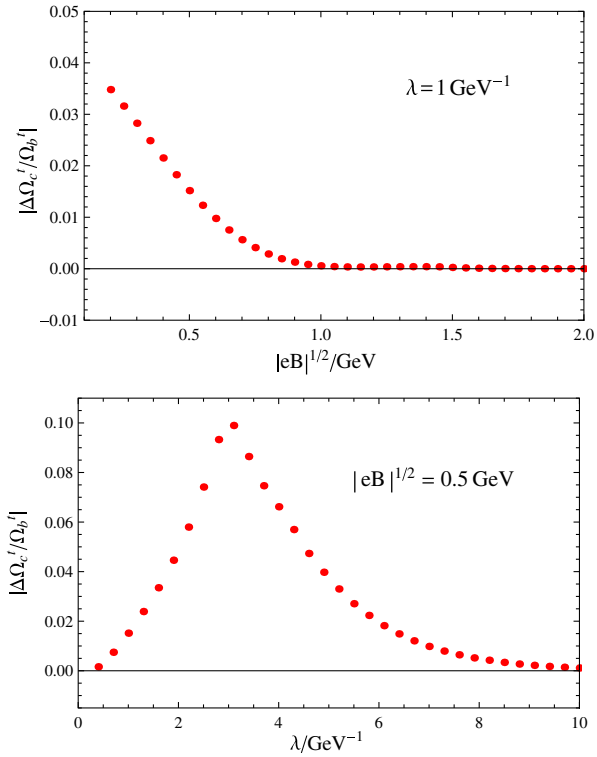

FIG. 2. The ratio $\Delta\Omega_c^t/\Omega_b^t$, where the color and flavor degrees of freedom are both taken into account, as a function of the magnetic field magnitude B for a given scale λ (upper panel) and of λ for a given B (lower panel). The chemical potential, temperature, and mass are reasonably chosen as $\mu = 0$, $T = 0.15$ GeV, and $m = 0.3$ GeV.

$$\Omega_B^t = \Omega_b^t + \Delta\Omega_c^t, \tag{18}$$

which vanishes at $B = 0$. In order to explore the relative importance of the discrete and continuum eigenstates, we compute the ratio $\Delta\Omega_c^t/\Omega_b^t$ in this part for convenience. As shown in Fig. 2, the contribution from the continuum part is usually very small compared to the discrete one and can be neglected for simplicity, which justifies the later treatment in the weak magnetic-field approximation. Finally, by recovering the B-independent term or the thermodynamic potential in the $B = 0$ case, which takes the following three-momentum cutoff regularized form [42],

$$\begin{aligned}\Omega_\Lambda(m,T,\mu) = &-\frac{T}{\pi^2}\sum_{s=\pm}\int_0^\infty p^2 dp \ln(1+e^{-(E(p)+s\mu)/T}) \\ &-\frac{m^3}{8\pi^2}\left[\Lambda\left(1+\frac{2\Lambda^2}{m^2}\right)\sqrt{1+\frac{\Lambda^2}{m^2}}\right. \\ &\left.-m\ln\left(\frac{\Lambda}{m}+\sqrt{1+\frac{\Lambda^2}{m^2}}\right)\right],\end{aligned} \tag{19}$$

the total finite thermodynamic potential of the NJL model in the given semilocalized magnetic field is

$$\Omega = \frac{(m-m_0)^2}{4G} + N_c\sum_{\mathrm{f=u,d}}(\Omega_\Lambda + \Omega_B + \Omega_B^t). \tag{20}$$

Now, if we fix the system size L, which is large enough to neglect boundary effect, then only the case $\lambda \gtrsim L$ is interesting for such a system because the average effect of the magnetic field is not vanishingly small. In this case, N_s is usually very large, and the contribution from the continuum spectrum can be safely neglected due to either the heaviness or the relatively small effective integral region of p_2. Then, the thermodynamic potential can be simply given by $\Omega_b(m^2, q_\mathrm{f}, B, \lambda, T, \mu)$ with the integral limit of p_2 fixed as $\pm q_\mathrm{f}BL/2$ as stated before. Thus, it can be regularized in the more convenient Pauli-Villars scheme [15] as

$$\Omega = \frac{(m-m_0)^2}{4G} + N_c\sum_{\mathrm{f=u,d}}\sum_{j=0}^{2} C_j\Omega_b(m^2+j\Lambda^2, B, \lambda, T, \mu) \tag{21}$$

with $C_j = 3j^2 - 6j + 1$.

B. Weak magnetic field approximation

Due to the difficulty in determining the exact mass gap from the gap equation (5), we will try to solve this issue in the weak magnetic field limit. Here, "weak" actually just means the effect of the magnetic field is very small compared to the chiral condensate already developed in the vacuum. It is reasonable to expect that the coordinate-dependent part of the mass gap $m(x)$ is restricted to the same region, where the semilocalized magnetic field presents. Thus, "weak magnetic field" just means small $m(x)$, and we can make Taylor expansions of the thermodynamic potential to the second order of $m(x)$, that is,

$$\begin{aligned}\Omega = \frac{1}{V_4}\left[\int d^4X\frac{(m+m(x)-m_0)^2}{4G} - \mathrm{Tr}\ln G^{-1}(X,X)\right. \\ \left. + \mathrm{Tr}G(X,X)m(x) + \frac{1}{2}\mathrm{Tr}G(X,X')m(x')G(X',X)m(x)\right].\end{aligned} \tag{22}$$

Here, the inverse fermion propagator $G^{-1}(X,X') = i\not{\partial} + \mu\gamma^0 - m$ and the constant mass m should be determined in the case without magnetic field with the thermodynamic potential:

$$\Omega = \frac{(m-m_0)^2}{4G} - \frac{N_cN_f}{V_4}\mathrm{tr}\ln(i\not{\partial} + \mu\gamma^0 - m). \tag{23}$$

From the explicit regularized expression Eq. (19), we have the following gap equation [42]:

$$\frac{m-m_0}{2G}=\frac{N_c m^2}{\pi^2}\left[\Lambda\sqrt{1+\frac{\Lambda^2}{m^2}}-m\ln\left(\frac{\Lambda}{m}+\sqrt{1+\frac{\Lambda^2}{m^2}}\right)\right]-\frac{N_c m}{\pi^2}\sum_{s=\pm}\int_0^\infty p^2dp\frac{1}{E(p)}\frac{2}{1+e^{(E(p)+s\mu)/T}}. \tag{24}$$

Then the extremal condition $\delta\Omega/\delta m(x)=0$ gives the following integral equation:

$$\frac{m+m(x)-m_0}{2G}+\int\frac{d^3p}{(2\pi)^3}\mathrm{tr}G(p;x,x)+\int\frac{d^3p}{(2\pi)^3}\int dx'\mathrm{tr}G(p;x,x')m(x')G(p;x',x)=0, \tag{25}$$

where $\mathrm{tr}G(p;x,x)$ can be evaluated by following the property

$$\begin{aligned}\mathrm{tr}(i\not{D}+\mu\gamma^0-m)^{-1}&=\mathrm{tr}(i(\omega_l+i\mu)\gamma^0-i\not{D}_i-m)[(\omega_l+i\mu)^2-D_i^2+m^2+q_\mathrm{f}\sigma_{\mu\nu}F^{\mu\nu}]^{-1}\\&=-m\mathrm{tr}[(\omega_l+i\mu)^2-D_i^2+m^2+q_\mathrm{f}\sigma_{\mu\nu}F^{\mu\nu}]^{-1}\end{aligned} \tag{26}$$

as [29,30]

$$\begin{aligned}\mathrm{tr}G(p;x,x)&=-\frac{2m}{W}\sum_{s=\pm}g_1(s,x)g_2(s,x),\qquad W=\frac{2}{\lambda}\frac{\Gamma(1+2a)\Gamma(1+2b)}{\Gamma(a+b+\frac{1}{2}-c_s)\Gamma(a+b+\frac{1}{2}+c_s)},\\g_1(s,x)&=\xi^a(1-\xi)^bF\left(a+b+\frac{1}{2}-c_s,a+b+\frac{1}{2}+c_s;1+2a;\xi\right),\\g_2(s,x)&=\xi^a(1-\xi)^bF\left(a+b+\frac{1}{2}-c_s,a+b+\frac{1}{2}+c_s;1+2b;1-\xi\right),\qquad\xi=\frac{1+\tanh(\frac{x}{\lambda})}{2}\\a&=\frac{\lambda}{2}\sqrt{(p_2-q_\mathrm{f}B\lambda)^2+(\omega_l+i\mu)^2+p_3^2+m^2},\qquad b=\frac{\lambda}{2}\sqrt{(p_2+q_\mathrm{f}B\lambda)^2+(\omega_l+i\mu)^2+p_3^2+m^2}.\end{aligned} \tag{27}$$

In the limit $B\to0$, $F(a+b+\frac{1}{2}-c_s,a+b+\frac{1}{2}+c_s;1+2a;\xi)\to(1-\xi)^{-2a}$ and the trace reduces to $-2m/\sqrt{p_2^2+(\omega_l+i\mu)^2+p_3^2+m^2}$, which is consistent with the usual one obtained in energy-momentum space, but p_1 is integrated over first here. In the limit $x\to\infty$ or $\xi\to1$, the hypergeometric functions become

$$\begin{aligned}F\left(a+b+\frac{1}{2}-c_s,a+b+\frac{1}{2}+c_s;1+2a;\xi\right)&=\frac{(1-\xi)^{-2b}}{2b}\frac{\Gamma(1+2a)\Gamma(1+2b)}{\Gamma(a+b+\frac{1}{2}-c_s)\Gamma(a+b+\frac{1}{2}+c_s)},\\F\left(a+b+\frac{1}{2}-c_s,a+b+\frac{1}{2}+c_s;1+2b;1-\xi\right)&=1.\end{aligned} \tag{28}$$

Then $\mathrm{tr}G(p;x,x)$ becomes magnetic field independent after shifting the integral variable p_2 in b which indicates $\lim_{x\to\infty}m(x)=0$ as expected. For the last term on the left-hand side of the gap equation (25), the effective integral region is constrained by $m(x)$, or originally by $B(x)$, to order λ. Thus, for not too large λ, it is enough to evaluate this term with the fermion propagator in the absence of magnetic field because that only gives the next-to-next-to-next- order contribution, and we can just take $m(x')\approx m(x)$ as its leading order contribution of the Taylor expansions around x. Finally, the integral equation (25) can be reduced to an algebra equation:

$$m(x)=-\left[\frac{1}{2G}+\int\frac{d^4p}{(2\pi)^4}\mathrm{tr}(i(\omega_l+i\mu)\gamma^0+p^i\gamma^i-m)^{-2}\right]^{-1}\left[\int\frac{d^3p}{(2\pi)^3}\mathrm{tr}G(p;x,x)-(B\to0)\right]. \tag{29}$$

The prefactor in the expression of $m(x)$ is actually the propagator of the σ mode at vanishing energy-momentum and can be given directly as [34]

$$\begin{aligned}&\left[\frac{1}{2G}+\int\frac{d^4p}{(2\pi)^4}\mathrm{tr}(i(\omega_l+i\mu)\gamma^0+p^i\gamma^i-m)^{-2}\right]^{-1}\\&\quad=\left[\frac{1}{2G}-N_cN_f\int_0^\Lambda\frac{dp}{\pi^2}\frac{p^4}{E^3(p)}+N_cN_f\sum_{s=\pm}\int_0^\infty\frac{dp}{\pi^2}\frac{p^4}{E^3(p)}\frac{1}{1+e^{(E(p)+s\mu)/T}}\right]^{-1}.\end{aligned} \tag{30}$$

In principle, the magnetic-field-dependent part needs further regularization as the prefactor, but the integral over p_2 is automatically constrained for not too large λ, as will be shown in the following.

According to the properties of the hypergeometric function, there is no pole in $g_1(s,x)g_2(s,x)$ for $0<\xi<1$. Thus, the poles of $\mathrm{tr}G(p;x,x)$ solely come from $\Gamma(a+b+\frac{1}{2}-|c_s|)$ for $a+b+\frac{1}{2}-|c_s|=-n(n\in\mathbb{Z})$, which correspond to the discrete spectra. Thus, the summation over the Matsubara frequency can be completed to give

$$\int\frac{d^3p}{(2\pi)^3}\mathrm{tr}G(p;x_1,x_1)=-\frac{2}{\lambda}\sum_{s,t=\pm}\int\frac{d^2p}{(2\pi)^2}\sum_{n=0}^{N_s}\frac{m\Gamma(2|c_s|-n)}{\Gamma(1+2a_n^s)\Gamma(1+2b_n^s)}\frac{(-1)^n}{n!}\frac{a_n^sb_n^s}{|c_s|-\frac{1}{2}-n}\xi^{2a_n^s}(1-\xi)^{2b_n^s}\frac{\tanh(\frac{E_{ns}(p_2,p_3,m)+t\mu}{2T})}{E_{ns}(p_2,p_3,m)}$$
$$\times F(-n,2|c_s|-n;1+2a_n^s;\xi)F(-n,2|c_s|-n;1+2b_n^s;1-\xi),\tag{31}$$

where the discrete a_n^s and b_n^s are, respectively,

$$a_n^s=\frac{1}{2}\left|\left(n+\frac{1}{2}-|c_s|\right)-(p_2q_fB\lambda^3)\left(n+\frac{1}{2}-|c_s|\right)^{-1}\right|,$$
$$b_n^s=\frac{1}{2}\left|\left(n+\frac{1}{2}-|c_s|\right)+(p_2q_fB\lambda^3)\left(n+\frac{1}{2}-|c_s|\right)^{-1}\right|.\tag{32}$$

As has been mentioned, the contribution from discrete spectra vanishes automatically at zero magnetic field because $N_s<0$. From the non-negativity of N_s, the integral limits of p_2 are found to be constrained as $\pm(c_s-3/2)^2/|q_fB\lambda^3|$, which serve as natural momentum cutoffs if λ is not so large. The integral over p_3 is divergent which can be regularized by the three-momentum cutoff Λ for simplicity. Still, there is a contribution from the continuum spectra which can be neglected after separating out the B-independent part, as indicated in the previous section.

As a byproduct, the magnetic-field-dependent term can be derived directly by neglecting the degree of freedom along p_3 in $2+1$ dimensions, that is,

$$\int\frac{d^2p}{(2\pi)^2}\mathrm{tr}G(p;x,x)=-\frac{2}{\lambda}\sum_{s,t=\pm}\int\frac{dp_2}{2\pi}\sum_{n=0}^{N_s}\frac{m\Gamma(2|c_s|-n)}{\Gamma(1+2a_n^s)\Gamma(1+2b_n^s)}\frac{(-1)^n}{n!}\frac{a_n^sb_n^s}{|c_s|-\frac{1}{2}-n}\xi^{2a_n^s}(1-\xi)^{2b_n^s}\frac{\tanh(\frac{E_{ns}(p_2,0,m)+t\mu}{2T})}{E_{ns}(p_2,0,m)}$$
$$\times F(-n,2|c_s|-n;1+2a_n^s;\xi)F(-n,2|c_s|-n;1+2b_n^s;1-\xi).\tag{33}$$

Then, as we have already known, the prefactor in the gapped phase at zero temperature [41] is

$$\left[\frac{1}{2G}+\int\frac{d^3p}{(2\pi)^3}\mathrm{tr}(i\omega\gamma^0+p^i\gamma^i-m)^{-2}\right]^{-1}=\frac{\pi}{m},\tag{34}$$

and the mass fluctuation Eq. (29) is simply reduced to

$$m(x)=\frac{2}{\lambda}\sum_{s=\pm}\int dp_2\sum_{n=0}^{N_s}\frac{\Gamma(2|c_s|-n)}{\Gamma(1+2a_n^s)\Gamma(1+2b_n^s)}\frac{(-1)^n}{n!}\frac{a_n^sb_n^s}{|c_s|-\frac{1}{2}-n}\frac{\xi^{2a_n^s}(1-\xi)^{2b_n^s}}{E_{ns}(p_2,0,m)}$$
$$F(-n,2|c_s|-n;1+2a_n^s;\xi)F(-n,2|c_s|-n;1+2b_n^s;1-\xi).\tag{35}$$

Thus, for second-order transitions such as those induced by coupling tuning, local chiral symmetry breaking with $m(x)\neq 0$ will be realized; but for first-order transitions such as those induced by chemical potential, $m(x)\propto m$ due to the invalidity of Eq. (34), local chiral symmetry is also restored.

III. NUMERICAL RESULTS

We devote this section primarily to exploring the coordinate-dependent mass fluctuation $m(x)$ briefly in $2+1$ dimensions and, in detail, in $3+1$ dimensions. In $2+1$ dimensions, there is only one energy scale, m_g, in the vacuum, so we take m_g as the unit of all other dimensional quantities for universality. In $3+1$ dimensions, the parameters of the NJL model were fixed to $G=4.93\ \mathrm{GeV}^{-2}$, $\Lambda=0.653\ \mathrm{GeV}$, and $m_0=5\ \mathrm{MeV}$ by fitting the pion mass $m_\pi=134\,\mathrm{MeV}$, pion decay constant $f_\pi=93\,\mathrm{MeV}$, and quark condensate $\langle\bar{\psi}\psi\rangle=-2\times(0.25\ \mathrm{GeV})^3$ in the vacuum [43].

It is instructive to qualitatively illuminate the effects of the magnitude B and scale λ of the magnetic field to chiral symmetry breaking and restoration in the constant m *Ansätz*. The gap equations can be derived from the thermodynamic potentials Eqs. (15) and (20) through

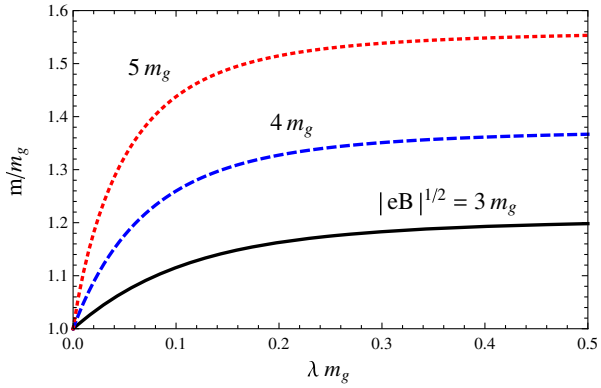

FIG. 3. The mass m as a function of the magnetic field scale λ for fixed magnitude B at zero temperature in $2+1$ dimensions with supercritical coupling $g > g_c$. All the quantities are scaled by m_g to dimensionless ones.

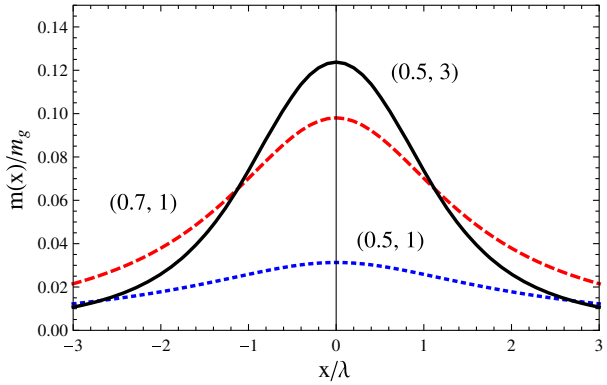

FIG. 5. The mass gap $m(x)$ in the region where the magnetic field is localized in $2+1$ dimensions at zero temperature and baryon chemical potential. The parameters shown in the plot are $(|eB|^{1/2}/m_g, \lambda m_g)$.

$\partial\Omega/\partial m = 0$ for $2+1$ and $3+1$ dimensions, respectively. The results are shown in Figs. 3 and 4, from which both chiral catalysis effects of B and λ can be easily identified.

Then, for more reasonable study of local chiral symmetry breaking and restoration, the $2+1$-dimensional results are illuminated in Fig. 5 for the supercritical case $g > g_c$. As we can see, the weak magnetic field approximation is still good for the magnetic field comparable to m_g and the magnetic catalysis effect shows up for the local chiral symmetry breaking. Besides, the larger magnetic field scale λ usually means a higher peak but smaller half-width of $m(x)$. It can be understood in this way: For larger λ, the region near the original is more like in a constant magnetic field, which of course prefers a larger $m(0)$ due to MCE. However, the magnitude at the boundary, $m(\pm 3\lambda)$, is not sensitive to λ due to the flatness of $B(x)$ there (see the upper panel of Fig. 1), which then just means the reduction of the half-width. All the features are qualitatively consistent with the ones obtained in a constant m *Ansätz* (Fig. 3).

The $3+1$-dimensional results are illuminated in Fig. 6, share similar features as the results of the $2+1$-dimensional case, and are qualitatively consistent with the ones obtained with the constant m *Ansätz* (Fig. 4). Finally, in order to explicitly show how the local mass fluctuation responds to the global chiral symmetry restoration, we calculate the constant mass m together with the original mass fluctuation $m(0)$ at different temperature and chemical potential; see Fig. 7. As is illuminated, the fluctuation is not sensitive to the change of m when it is still considerably large and is deeply suppressed when it becomes small, which justifies the Taylor expansions in the whole region. It is interesting that the ratio $m(0)/m$ would show a peak ~ 0.4 around the critical temperature, which is just an indication of phase transition. Because of the approximate chiral symmetry with finite current quark mass and

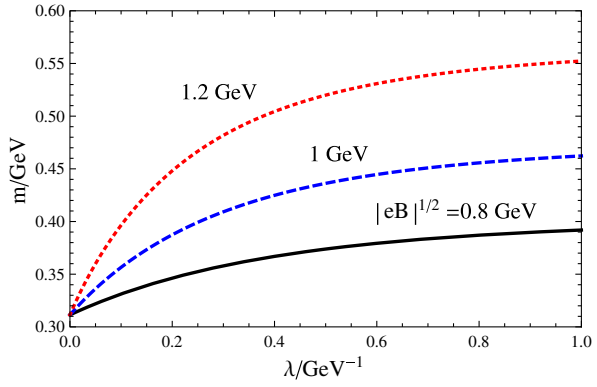

FIG. 4. The mass m as a function of the magnetic field scale λ for fixed magnitude B at zero temperature in the $3+1$-dimensonal NJL model.

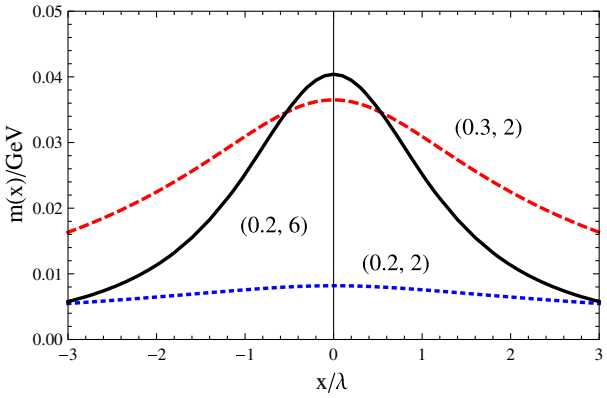

FIG. 6. The mass gap $m(x)$ in the region where the magnetic field is localized in $3+1$ dimensional NJL model at zero temperature and baryon chemical potential. The parameters shown in the plot are $(|eB|^{1/2}, \lambda)$ in the unit $(\mathrm{GeV}, \mathrm{GeV}^{-1})$.

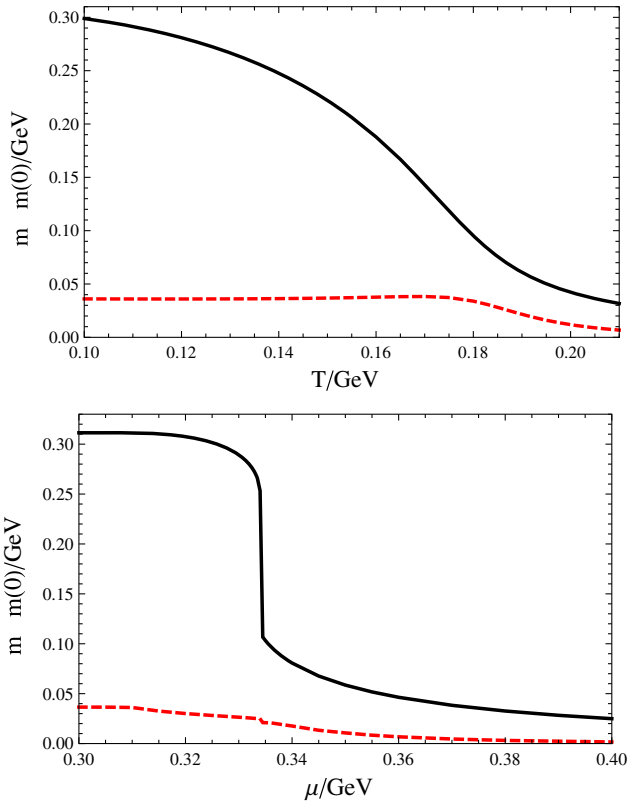

FIG. 7. The constant mass gap m (black solid lines) and the maximal fluctuation $m(0)$ (red dashed lines) as functions of temperature T at vanishing baryon chemical potential (upper panel) and baryon chemical potential μ at vanishing temperature in the $3+1$-dimensional NJL model. The magnitude and scale of the magnetic field are chosen as $(|eB|^{1/2}, \lambda) = (0.3\ \mathrm{GeV}, 2\ \mathrm{GeV}^{-1})$.

nonrenormalizability with four fermion couplings of the NJL model, the expected features across the phase transition for $2+1$ dimensions are not found. In particular, the vanishing of $m(x)$ is not found across the first-order transition because m is still finite after the transition.

IV. CONCLUSIONS

In this work, we first developed a formalism to evaluate the thermodynamic potential with constant fermion mass in the region where the magnetic field is localized and also for the system with fixed size under the framework of the NJL model. Then apart from the magnetic-field-independent terms, the contributions from the discrete and continuum spectra were compared with each other, which indicates the negligible of the latter. Finally, we tried to study the local chiral symmetry breaking due to a weak semilocalized magnetic field by using the Taylor expansion technique, which is the main motivation of this work.

The main findings are the following. In the constant m *Ansätz*, both the magnetic field magnitude B and scale λ tend to catalyze chiral symmetry breaking in the $2+1$- and $3+1$-dimensional cases. And in the weak magnetic field approximation, the local chiral condensate was also found to be enhanced by both B and λ, which confirms the qualitative features from the constant m *Ansätz*. Thus, the results indicate the importance of inhomogeneous magnetic field effect in HICs with much larger B and that the expanding of the fireball (λ becomes larger) doesn't necessarily reduce the magnetic field effect during the period when B sustains. Furthermore, the mass fluctuation $m(x)$ is found to be not sensitive to the change of temperature T or baryon chemical potential μ when the global mass is still considerably large, which further supports the importance of the inhomogeneous magnetic effect in HICs.

ACKNOWLEDGMENTS

We thank Xu-guang Huang from Fudan University for his comments on this work. G. C. is supported by the Thousand Young Talents Program of China, Shanghai Natural Science Foundation with Grant No. 14ZR1403000, the NSFC with Grants No. 11535012 and No. 11675041, and the China Postdoctoral Science Foundation with Grant No. KLH1512072.

[1] V. Skokov, A. Y. Illarionov, and V. Toneev, Estimate of the magnetic field strength in heavy-ion collisions, Int. J. Mod. Phys. A **24**, 5925 (2009).
[2] V. Voronyuk, V. D. Toneev, W. Cassing, E. L. Bratkovskaya, V. P. Konchakovski, and S. A. Voloshin, (Electro-)Magnetic field evolution in relativistic heavy-ion collisions, Phys. Rev. C **83**, 054911 (2011).
[3] A. Bzdak and V. Skokov, Event-by-event fluctuations of magnetic and electric fields in heavy ion collisions, Phys. Lett. B **710**, 171 (2012).
[4] W. T. Deng and X. G. Huang, Event-by-event generation of electromagnetic fields in heavy-ion collisions, Phys. Rev. C **85**, 044907 (2012).
[5] G. S. Bali, F. Bruckmann, G. Endrodi, Z. Fodor, S. D. Katz, S. Krieg, A. Schafer, and K. K. Szabo, The QCD phase diagram for external magnetic fields, J. High Energy Phys. 02 (2012) 044.
[6] G. S. Bali, F. Bruckmann, G. Endrodi, Z. Fodor, S. D. Katz, and A. Schafer, QCD quark condensate in external magnetic fields, Phys. Rev. D **86**, 071502 (2012).

[7] F. Bruckmann, G. Endrodi, and T. G. Kovacs, Inverse magnetic catalysis and the Polyakov loop, J. High Energy Phys. 04 (2013) 112.
[8] G. Endrodi, Critical point in the QCD phase diagram for extremely strong background magnetic fields, J. High Energy Phys. 07 (2015) 173.
[9] K. Fukushima and Y. Hidaka, Magnetic Catalysis Versus Magnetic Inhibition, Phys. Rev. Lett. **110**, 031601 (2013).
[10] J. Chao, P. Chu, and M. Huang, Inverse magnetic catalysis induced by sphalerons, Phys. Rev. D **88**, 054009 (2013).
[11] B. Feng, D. F. Hou, and H. C. Ren, Magnetic and inverse magnetic catalysis in the Bose-Einstein condensation of neutral bound pairs, Phys. Rev. D **92**, 065011 (2015).
[12] G. Cao, L. He, and P. Zhuang, Collective modes and Kosterlitz-Thouless transition in a magnetic field in the planar Nambu-Jona-Lasino model, Phys. Rev. D **90**, 056005 (2014).
[13] N. Mueller and J. M. Pawlowski, Magnetic catalysis and inverse magnetic catalysis in QCD, Phys. Rev. D **91**, 116010 (2015).
[14] X. Guo, S. Shi, N. Xu, Z. Xu, and P. Zhuang, Magnetic field effect on charmonium production in high energy nuclear collisions, Phys. Lett. B **751**, 215 (2015).
[15] G. Cao and P. Zhuang, Effects of chiral imbalance and magnetic field on pion superfluidity and color superconductivity, Phys. Rev. D **92**, 105030 (2015).
[16] G. Cao and X. G. Huang, Electromagnetic triangle anomaly and neutral pion condensation in QCD vacuum, Phys. Lett. B **757**, 1 (2016).
[17] C. Bonati, M. D'Elia, M. Mariti, M. Mesiti, F. Negro, A. Rucci, and F. Sanfilippo, Magnetic field effects on the static quark potential at zero and finite temperature, Phys. Rev. D **94**, 094007 (2016).
[18] V. A. Miransky and I. A. Shovkovy, Quantum field theory in a magnetic field: From quantum chromodynamics to graphene and Dirac semimetals, Phys. Rep. **576**, 1 (2015).
[19] Q. Li, D. E. Kharzeev, C. Zhang, Y. Huang, I. Pletikosić, A. V. Fedorov, R. D. Zhong, J. A. Schneeloch, G. D. Gu, and T. Valla, Observation of the chiral magnetic effect in ZrTe5, Nat. Phys. **12**, 550 (2016).
[20] K. Hattori and Y. Yin, Charge Redistribution from Anomalous Magnetovorticity Coupling, Phys. Rev. Lett. **117**, 152002 (2016).
[21] Z. Qiu, G. Cao, and X. G. Huang, On electrodynamics of chiral matter, Phys. Rev. D **95**, 036002 (2017).
[22] X. G. Huang, Y. Yin, and J. Liao, In search of chiral magnetic effect: Separating flow-driven background effects and quantifying anomaly-induced charge separations, Nucl. Phys. **A956**, 661 (2016).
[23] Y. Jiang, X. G. Huang, and J. Liao, Chiral vortical wave and induced flavor charge transport in a rotating quark-gluon plasma, Phys. Rev. D **92**, 071501 (2015).
[24] Y. Jiang, S. Shi, Y. Yin, and J. Liao, Quantifying chiral magnetic effect from anomalous-viscous fluid dynamics, Chin. Phys. C **42**, 011001 (2018).
[25] J. Liao, Anomalous transport effects, and possible environmental symmetry violation in heavy-ion collisions, Pramana **84**, 901 (2015).
[26] D. E. Kharzeev, Topology, magnetic field, and strongly interacting matter, Annu. Rev. Nucl. Part. Sci. **65**, 193 (2015).
[27] X. G. Huang, Electromagnetic fields, and anomalous transports in heavy-ion collisions—A pedagogical review, Rep. Prog. Phys. **79**, 076302 (2016).
[28] D. E. Kharzeev, J. Liao, S. A. Voloshin, and G. Wang, Chiral magnetic and vortical effects in high-energy nuclear collisions-A status report, Prog. Part. Nucl. Phys. **88**, 1 (2016).
[29] D. Cangemi, E. D'Hoker, and G. V. Dunne, Effective energy for QED in $(2+1)$-dimensions with semilocalized magnetic fields: A Solvable model, Phys. Rev. D **52**, R3163 (1995).
[30] G. V. Dunne and T. M. Hall, An Exact $(3+1)$-Dimensional QED Effective Action, Phys. Lett. B **419**, 322 (1998).
[31] P. Copinger and K. Fukushima, Spatially Assisted Schwinger Mechanism and Magnetic Catalysis, Phys. Rev. Lett. **117**, 081603 (2016).
[32] Y. Nambu and G. Jona-Lasinio, Dynamical model of elementary particles based on an analogy with superconductivity. 1., Phys. Rev. **122**, 345 (1961).
[33] Y. Nambu and G. Jona-Lasinio, Dynamical model of elementary particles based on an analogy with superconductivity. Ii, Phys. Rev. **124**, 246 (1961).
[34] S. P. Klevansky, The Nambu-Jona-Lasinio model of quantum chromodynamics, Rev. Mod. Phys. **64**, 649 (1992).
[35] D. T. Son and M. A. Stephanov, Axial anomaly and magnetism of nuclear and quark matter, Phys. Rev. D **77**, 014021 (2008).
[36] J. A. Bowers and K. Rajagopal, The crystallography of color superconductivity, Phys. Rev. D **66**, 065002 (2002).
[37] D. Nickel, How Many Phases Meet at the Chiral Critical Point?, Phys. Rev. Lett. **103**, 072301 (2009).
[38] G. Cao, L. He, and P. Zhuang, Solid-state calculation of crystalline color superconductivity, Phys. Rev. D **91**, 114021 (2015).
[39] G. Cao and L. He, Ginzburg-Landau free energy of crystalline color superconductors: A matrix formalism from solid-state physics, Commun. Theor. Phys. **64**, 687 (2015).
[40] G. Cao and A. Huang, Solitonic modulation and Lifshitz point in an external magnetic field within Nambu-Jona-Lasinio model, Phys. Rev. D **93**, 076007 (2016).
[41] B. Rosenstein, B. Warr, and S. H. Park, Dynamical symmetry breaking in four Fermi interaction models, Phys. Rep. **205**, 59 (1991).
[42] G. Cao and X. G. Huang, Chiral phase transition and Schwinger mechanism in a pure electric field, Phys. Rev. D **93**, 016007 (2016).
[43] P. Zhuang, J. Hufner, and S. P. Klevansky, Thermodynamics of a quark—meson plasma in the Nambu-Jona-Lasinio model, Nucl. Phys. **A576**, 525 (1994).